Journal of Power Sources 189 (2009) 344–352

Contents lists available at ScienceDirect

Journal of Power Sources

journal homepage: www.elsevier.com/locate/jpowsour

High voltage spinel oxides for Li-ion batteries: From the material research to the application

Sébastien Patoux*, Lise Daniel, Carole Bourbon, Hélène Lignier, Carole Pagano, Frédéric Le Cras, Séverine Jouanneau, Sébastien Martinet

CEA/LITEN, Commissariat à l'Energie Atomique/Laboratoire d'Innovation pour les Technologies des Energies Nouvelles, 17 rue des Martyrs, 38054 Grenoble Cedex 9, France

ARTICLE INFO

Article history:
Received 25 July 2008
Received in revised form 13 August 2008
Accepted 14 August 2008
Available online 27 August 2008

Keywords:
'3 V' and '5 V' Li-ion batteries
High energy
High power
Positive electrode materials
High voltage spinel oxides

ABSTRACT

Li-ion batteries are already used in many nomad applications, but improvement of this technology is still necessary to be durably introduced on new markets such as electric vehicles (EVs), hybrid electric vehicles (HEVs) or eventually photovoltaic solar cells. Modification of the nature of the active materials of electrodes is the most challenging and innovative aspect. High voltage spinel oxides for Li-ion batteries, with general composition $LiMn_{2-x}M_xO_4$ (M a transition metal element), may be used to face increasing power source demand. It should be possible to obtain up to 240 Wh kg^{-1} at cell level when combining a nickel manganese spinel oxide with graphite (even more with silicon/carbon nanocomposites at the anode). Specific composition and material processing have to be selected with care, as discussed in this paper. It is demonstrated that '$LiNi_{0.5}Mn_{1.5}O_4$' and $LiNi_{0.4}Mn_{1.6}O_4$ have remarkable properties such as high potential, high energy density, good cycle life and high rate capability. Choice of the electrolyte is also of primary importance in order to prevent its degradation at high voltage in contact with active surfaces. We showed that a few percents of additive in the electrolyte were suitable for protecting the positive electrode/electrolyte interface, and reducing the self-discharge. High voltage materials are also possibly interesting to be used in safe and high power Li-ion cells. In this case, the negative electrode may be made of $Li_4Ti_5O_{12}$ or TiO_2 to give a '3 V' system.

1. Introduction

Li-ion batteries are one of the solutions to meet the energy storage required and contributed to reduce the overall warming (greenhouse gases). These systems will probably compete with Ni–MH batteries for propulsion of hybrid electric vehicles in the next few years (2009–2015). They could also compete with lead–acid batteries for the storage of solar energy (photovoltaic cells). For these two major applications, as well as for portable electronics and upcoming applications, it is essential to further improve current Li-ion batteries (security, cost, performances). Present developments are aimed – through the search for new active compounds (electrodes and electrolyte) and implementation of optimized architectures – to improve the energy densities and power, security organs, while considering the cheapest and environmentally friendly solutions. In addition, the use of active materials conferring high energy densities allows to limit their amount, which normally saves energy at the level of their production and recycling.

Since the first Li-ion cells were introduced on the market by Sony in the early 1990s, worldwide researches have been performed to find better active materials (cost, safety, capacity, cycle life, etc.). Today, high energy commercial cells have energy density of about 200 Wh kg^{-1}. Most of the Li-ion cells are still using $LiCoO_2$ or $Li(Ni,Mn,Al,Co)O_2$ layered oxides at the positive electrode, and carbon graphite at the negative electrode. To compete with the layered oxides, high voltage spinel oxides have been studied for the last 10 years. Initially, these materials have been considered as substituted $LiMn_2O_4$ materials, because they were studied only for their 4 V capacity retention [1,2] (Mn^{4+}/Mn^{3+} redox couple). In 1997, Amine et al. [3] and Dahn and co-workers [4] envisioned the '5 V' component of $LiMn_{2-x}M_xO_4$ spinel oxides (M = Ni, Fe with $x = 0.5$, 1 and M = Ni with $0 < x < 0.5$). Subsequent researches have focused on simple or multi-substitutions for manganese to enhance the capacity at high voltage. For the last 6 years intensive efforts have been devoted to the development of $LiNi_{0.5}Mn_{1.5}O_4$ and variants as positive electrode materials for high energy density Li-ion batteries. In comparison with $LiMn_2O_4$, Mn remains essentially in the +4 oxidation state, under normal cycling conditions, avoiding complications associated with the Jahn–Teller distortion of Mn^{3+} ions in six-coordinate sites. The theoretical capacity of the $LiNi_{0.5}{}^{II}Mn_{1.5}{}^{IV}O_4/Ni_{0.5}{}^{IV}Mn_{1.5}{}^{IV}O_4$ redox system is 146.7 mAh g^{-1}.

* Corresponding author. Tel.: +33 4 38 78 29 20; fax: +33 4 38 78 51 98.
E-mail address: sebastien.patoux@cea.fr (S. Patoux).

0378-7753/$ – see front matter © 2008 Elsevier B.V. All rights reserved.
doi:10.1016/j.jpowsour.2008.08.043

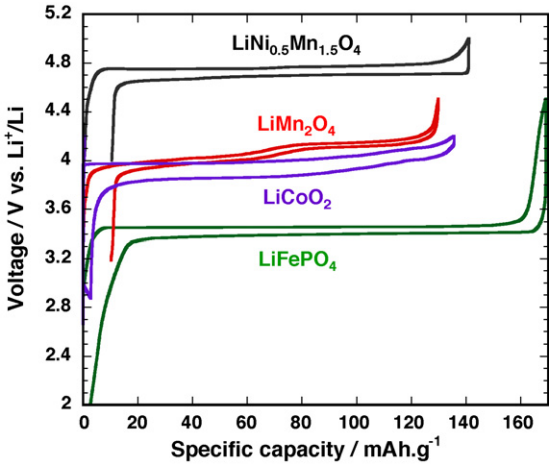

Fig. 1. Voltage vs. capacity for several positive electrode materials, obtained under normal cycling conditions (20 °C, *C*/5 rate).

It corresponds to the oxidation of nickel (II) in nickel (IV) at 4.7–4.75 V vs. Li^+/Li (Fig. 1). This high potential, in comparison with conventional $LiCoO_2$, $LiMn_2O_4$ and $LiFePO_4$, gives an energy density equivalent to 700 Wh kg^{-1} of active material, referring to Li metal.

For these reasons, $LiNi_{0.5}Mn_{1.5}O_4$ and substituted counterparts have focused large interest over the last 6 years, being depicted in more than 120 scientific papers. Subsequent researches for the last 4 years allowed us to optimize the electrochemical performances and highlight the $LiNi_{0.4}Mn_{1.6}O_4$ composition for future developments. This article will discuss our researches on the high voltage spinel oxides, and it will present the physico-chemical and electrochemical characterization of the best compounds. Self-discharge concerns will be presented. In a second part, the integration of $LiNi_{0.4}Mn_{1.6}O_4$ in Li-ion cells will be introduced. Depending on the nature of the negative electrode, high energy cells or safe and high power cells may be assembled.

2. Experimental

Spinel oxides were prepared by solid state reaction, starting from the respective carbonates in stoichiometric proportions ($MnCO_3$, $LiCO_3$ and $NiCO_3{\cdot}2Ni(OH)_2$). Pure powders (30 g batches) were obtained after mechanical activation (extensive ball-milling in hexane) and thermal treatments at 600 °C (10 h) and 900 °C (15 h) with specific cooling rate, usually 1.0° min^{-1}. A subsequent thermal treatment at 700 °C for several hours and a slow cooling rate (0.1° min^{-1}) is necessary to prepare the 'ordered' form of $LiNi_{0.5}Mn_{1.5}O_4$. In all cases, we developed an easy post-treatment in aqueous solution to improve the electrochemical performances of materials. One of the effects of this final stage is to tailor the particles by allowing separation of agglomerated particles. All the steps of the synthesis method are easily up-scalable.

X-ray diffraction (XRD) patterns at 300 K were obtained on a Bruker D8 diffractometer (θ–2θ geometry, back monochromator) using Cu Kα radiation (λ = 1.54056 Å). Neutron diffraction was also performed on several compounds. Experiments were carried out on the high-resolution D1A diffractometer of the Institute Laue-Langevin (ILL, Grenoble, France) at room temperature with wavelength 1.3898 Å, step 0.1° (θ, 2θ), and the data acquisition time of 8 h for each sample. Diffraction patterns were refined with the WinPLOTR/Fullprof suite [5]. Scanning electronic microscopy images were obtained with a XL30 Philips microscope. Specific surface measurements of powders were recorded with a Beckman Coulter analyser (BET method) after degassing at 300 °C for 4 h. Particle sizes distribution of samples was controlled by laser diffraction using Mastersizer S analyser from Malvern Instruments. Differential scanning calorimetry measurements were carried out on a Setsys system (Setaram, France).

Unless otherwise specified, basic electrochemical tests that are presented in this paper have been realized in 2032 type button cells, using thin composite positive electrodes prepared by thoroughly mixing 80 wt.% of active material (spinel oxides) with 10 wt.% Super P carbon black (Timcal) and 10 wt.% PVdF binder (polyvinylidene difluoride - Solef 1015, Solvay) in NMP (*N*-methyl-pyrrolidone). As-prepared inks were spread onto aluminum foils using a doctor blade, with a 100 μm gap. Electrodes (1.54 cm^2 discs), with loading of ~5 mg of active material (~0.4–0.5 mAh cm^{-2}), were dried for 24 h at 55 °C, pressed (6.5 t cm^{-2}), then dried again for 48 h at 80 °C under vacuum. Coin cells were assembled in argon filled dry box (<1 ppm O_2/H_2O) with a microporous polypropylene separator (Celgard® 2400). The liquid electrolyte used consisted in mixture of ethylene carbonate, propylene carbonate and dimethylcarbonate (1:1:3 in weight), containing $LiPF_6$ as salt (1 mol L^{-1}). 135-μm thick lithium foil (ALDRICH) is used as counter electrode for materials characterization and preliminary tests on electrode development. Electrochemical lithium insertion/extraction was monitored either with a "MacPile" automatic cycling/data recording system (Biologic SA, Claix, France) operating in galvanostatic and potentiostatic modes (tests < 10 mA), or with an Arbin BT/HSP-2043 automatic cycling data recording system (Arbin, Texas, USA), operating in galvanostatic mode (up to 10 A).

3. Results

3.1. Physico-chemical characterizations

$LiNi_{0.5}Mn_{1.5}O_4$ and substituted counterparts have a cubic close-packed oxygen array similar to the relative $LiMn_2O_4$. Generic $LiNi_{0.5}Mn_{1.5}O_4$ can either crystallized in $P4_332$ (Ni/Mn ordering) or *Fd*-3*m* (Ni/Mn disordering) space group, depending on the synthesis conditions [6,7]. Contrary to X-ray, neutron diffraction, which benefits from different coherent scattering lengths of Mn and Ni (−3.73 fm and +10.3 fm, respectively), is a useful technique to determine such an ordering as well as the lithium distribution (e.g., restricted or not to the tetrahedral sites). Direct spinel oxides usually adopt the *Fd*-3*m* space group, with lithium ions located in tetrahedral 8a sites and transition metal elements filling the 16d octahedral sites. The particular Ni/Mn ratio (1/3) allows, under some synthesis conditions (e.g., very low cooling rate), a cationic ordering over two distinct octahedral positions, thus nesting the nickel ions in the 4a sites and manganese ions in the 12d sites (S.G.: $P4_332$). Disordered phase is often considered as non-stoichiometric, and occasionally expressed as $LiNi_{0.5}Mn_{1.5}O_{4-\delta}$. Oxygen vacancies have been related to the minor redox activity noticed at 4 V vs. Li^+/Li, which is related to the oxidation of Mn^{3+} into Mn^{4+}. Non-stoechiometric compound usually has $Li_xNi_{1-x}O$ rock-salt type impurities. Neutron diffraction experiments have confirmed that we succeeded to prepare the expected ordered $LiNi_{0.5}Mn_{1.5}O_4$ spinel, without any impurity (Table 1). Lattice parameter is in agreement with refinement of X-ray patterns (a = 8.167(1) Å). No oxygen vacancy and full site occupancies (Li^+ in 8c, Ni^{2+} in 4a, Mn^{4+} in 12d, and oxygen atoms in 8c and 24e sites) were detected.

However, our general synthesis conditions give a disordered phase with partial ordering and small impurities enclosed (Fig. 2). This '$LiNi_{0.5}Mn_{1.5}O_4$' sample contained about 27% of ordered phases (a = 8.165(3) Å), 70% of disordered phases (a = 8.174(1) Å) and 3% of $Li_{0.18}Ni_{0.82}O$ (a = 4.15(1) Å). This sample has better electrochemical performances than the well-ordered sample (cycling life, rate

Table 1
Summary of the X-ray and neutron diffraction refinements for ordered and disordered '$LiNi_{0.5}Mn_{1.5}O_4$' (cooled down at −0.1 and 1° min^{-1}, respectively) and $LiNi_{0.4}Mn_{1.6}O_4$ powders

Sample	Ordered phase (not shown)	Disordered phase (Fig. 2)	$LiNi_{0.4}Mn_{1.6}O_4$ (Fig. 3)
Composition	$LiNi_{0.5}Mn_{1.5}O_4$ (100%)	a. '$LiNi_{0.5}Mn_{1.5}O_4$' (70%) b. $LiNi_{0.5}Mn_{1.5}O_4$ (27%) c. $Li_{1-18}Ni_{0.82}O$ (3%)	$LiNi_{0.4}Mn_{1.6}O_4$ (100%)
Temperature (K)	293	293	293
Instrument	D1A at ILL (neutron)	D1A at ILL (neutron)	Bruker D8 (X-Ray)
Wavelength (Å)	1.3898	1.3898	1.54056
Space group (no.)	$P4_332$ (212)	a. *Fd*-3*m* (227) b. $P4_332$ (212) c. *Fm*-3*m* (225)	*Fd*-3*m* (227)
Lattice parameter (Å)	8.167(1)	a. 8.174(1) b. 8.165(3) c. 4.15(1)	8.180(1)
Volume ($Å^3$)	545(1)	a. 546(1) b. 544(1) c. 71(1)	547(1)
Z (formula units per cell)	8	a. 8 b. 8 c. 4	8
R_{Bragg} (%)	4.82	6.96	5.36

capability). We thus decided to proceed to extra calcinations at high temperature and faster cooling rates, like quenching, to further enhance disordering. We determined that such materials have worse cycling stability than our conventional material. It was attributed to the increase in oxygen vacancies and Mn^{3+} content, as refined. To reduce the ordering part without introducing too much vacancies and Mn^{3+} ions, other samples with compositions $Li_{(1+x/3)}Ni^{II}_{(0.5-x/2)}Mn^{IV}_{(1.5+x/6)}O_4$ were prepared using our conventional processing method. Analysis of neutron diffraction pattern of $Li_{1.033}Ni_{0.45}Mn_{1.517}O_4$ (i.e., $x = 0.1$) has been done. Contrary to what we thought, a partial transition metal ordering was detected (66% disordering and 33% ordering, with less than 1% rock-salt type impurity).

Subsequent researches performed in our laboratory allowed to optimize the electrochemical performance of the nickel manganese spinel oxides. We showed that appropriate post-synthesis treatment in aqueous solution improves the cycle life. This treatment does not modify the unit-cell parameter, the oxygen vacancies or the Ni/Mn ordering. Among the various compositions investigated (doped-, substituted- and modified-$LiNi_{0.5}Mn_{1.5}O_4$), we focused on the study of $LiNi_{0.4}Mn_{1.6}O_4$ ($a = 8.180(1)$ Å). This material is less oxygen sensitive, and it was obtained without any impurity (Fig. 3). It has very good electrochemical properties as presented in Section 3.2.

After completion of the post-treatment, all samples have specific surface area of ca. 1.0(1) $m^2\ g^{-1}$. Laser granulometry revealed particles with homogenous dispersion (Fig. 4) that avoids the use of jet-milling or other sieving techniques usually need before the elaboration of electrodes. All particles are usually between 1 and 30 μm size. Their morphology was observed by scanning electronic microscopy (insert of Fig. 3).

3.2. Electrochemical characterizations of the nickel manganese spinel oxides

In the literature, the disordered '$LiNi_{0.5}Mn_{1.5}O_4$' phase is the most familiar nickel manganese spinel oxide, due to better electrochemical performance than the ordered phase [8]. It is a non-stoichiometric compound, having Mn^{3+} ions as minor impu-

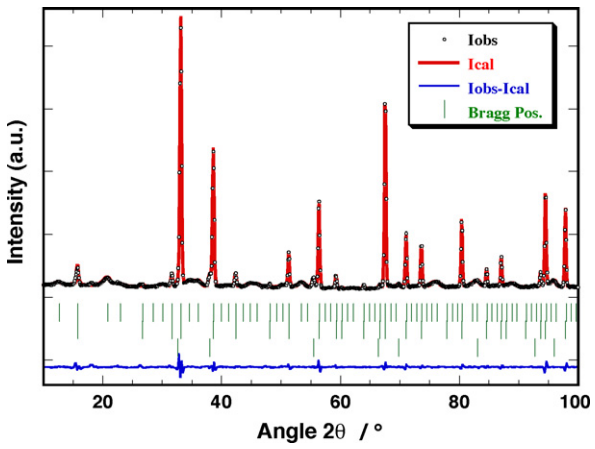

Fig. 2. Neutron diffraction pattern (λ = 1.3898 Å) and Rietveld refinement of our conventional '$LiNi_{0.5}Mn_{1.5}O_4$' spinel oxide. Bragg positions correspond, from top, to ordered spinel ($P4_332$), disordered spinel (*Fd*-3*m*) and $Li_xNi_{1-x}O$ rock-salt impurities ($x \sim 0.2$).

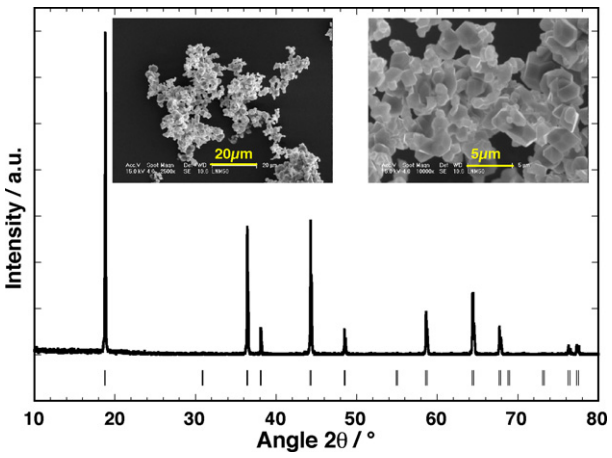

Fig. 3. X-ray diffraction pattern of $LiNi_{0.4}Mn_{1.6}O_4$ (Cu Kα radiation—λ = 1.54056 Å, θ–2θ geometry, back monochromator) with Bragg positions corresponding to *Fd*-3*m* space group ($a = 8.180$ Å). (Insert) Scanning electronic microscopy images of the particles distribution of $LiNi_{0.4}Mn_{1.6}O_4$ spinel oxide.

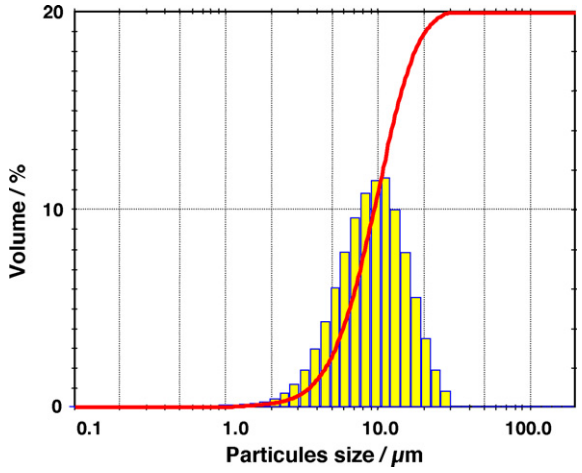

Fig. 4. Particle size distribution of $LiNi_{0.4}Mn_{1.6}O_4$ prepared from our conventional synthesis method, including the post-treatment.

rity. The oxidation of Mn^{3+} into Mn^{4+} gives a parasitic redox activity at 4 V vs. Li^+/Li (Fig. 5). At the opposite, ordered-$LiNi_{0.5}Mn_{1.5}O_4$ is a pure Mn^{4+} compound with no activity in the 4 V region. In all cases, Ni^{2+} ions are reversibly oxidized at 4.7–4.75 V vs. Li^+/Li. Depending on the ordering, one or two peaks (one or two two-phase domains) can be observed. In first approximation, the ordered phase exhibits a single phenomenon and a large ohmic drop between charge and discharge. For the disordered '$LiNi_{0.5}Mn_{1.5}O_4$' phase a separation into two redox 'plateaus' (two peaks), shifted by 50 mV, is well described. In the literature, mechanism of lithium insertion/extraction into/from ordered $LiNi_{0.5}Mn_{1.5}O_4$ was studied by Ozhuku co-workers [9]. From $x = 1$ to $x = 0$, two cubic/cubic two-phase reactions occur (at 4.72 and 4.74 V vs. Li^+/Li), with intermediate definite composition at $x = 0.5$. In agreement with Ni^{2+} oxidation into Ni^{3+}, then Ni^{4+}, the lattice parameter decreases from 8.17 to 8.00 Å. At the same time, Kim et al. investigated the structural changes for both ordered and disordered $LiNi_{0.5}Mn_{1.5}O_4$ [8,10], and observed distinct mechanisms. When ordered $LiNi_{0.5}Mn_{1.5}O_4$ shows topotactic phase transition among three different cubic phases upon lithium extraction (cations disordering operates during charge), disordered $LiNi_{0.5}Mn_{1.5}O_4$ exhibits one phase process from $x = 1$ to $x \sim 0.25$, then a two-phase process from $x \sim 0.25$ to $x = 0$ (both phases have cubic symmetry). According to Kim et al., ordered spinel has low structural reversibility and rapid capacity fading at

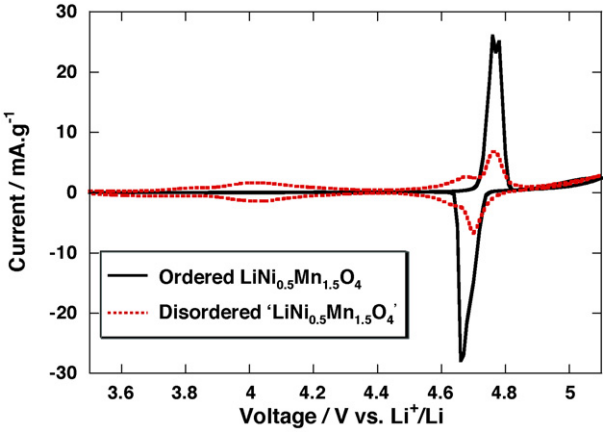

Fig. 5. Calculated incremental capacity voltammograms (derivative from galvanostatic curves at $C/5$ rate at 20 °C) for ordered and disordered '$LiNi_{0.5}Mn_{1.5}O_4$' spinel oxides vs. metallic lithium.

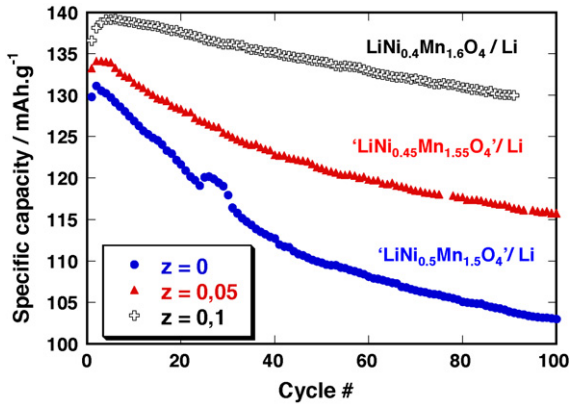

Fig. 6. Discharge capacity as a function of cycle number for $LiNi_{0.4}Mn_{1.6}O_4$/Li, '$LiNi_{0.45}Mn_{1.55}O_4$'/Li and '$LiNi_{0.5}Mn_{1.5}O_4$'/Li at $C/5$ rate (20 °C), between 3.5 and 5 V.

high rates. We also confirmed this remark, and surprisingly noticed a better ability for disordered spinel than for ordered spinel to preserve stable capacity upon cycling at normal rates ($\sim C/5$). In recent papers, Amatucci explained that disordered phase has two orders-of-magnitude higher lithium diffusion coefficient than the ordered counterpart [11,12]. Ordered phase is thus limited by its low electronic conductivity (10^{-7} S cm^{-1}). In accordance with the previous observations, presence of manganese Mn^{3+} ions seems to contribute to the conductivity enhancement and cycle life improvement. We decided to prepare samples with $LiNi_{0.5-y}Mn_{1.5+y}O_4$ ($y \leq 0.1$) compositions using our conventional synthesis method (without post-treatment at this stage). As far as the increase in the y value, the Mn^{3+} content increases and the rock-salt type impurity decreases. The evolution of the specific capacity vs. cycle number for three compositions (both limits and an intermediate) is reported in Fig. 6. As expected from our last results on '$LiNi_{0.5}Mn_{1.5}O_4$', the higher Mn^{3+} content, the better is the cycle life. At the opposite, the higher Mn^{3+} content, the lower is the average potential and energy density. A comparison of the energy density (Watt-hours per kilogram of active material) at various rates is given in Fig. 7. Although $LiNi_{0.4}Mn_{1.6}O_4$ have 0.2 mole of Mn^{3+} ions (4 V vs. Li^+/Li) and only 0.4 mol of Ni^{2+} ions (4.7 V vs. Li^+/Li), this compound has the best practical energy density at all rates. It is very close to the theoretical value at low rate (675 Wh kg^{-1}).

Electrolyte instability at high potential, particularly above 4.5 V vs. Li^+/Li, is a natural drawback when using high voltage spinel oxides. In order to reduce degradation of electrolyte and capac-

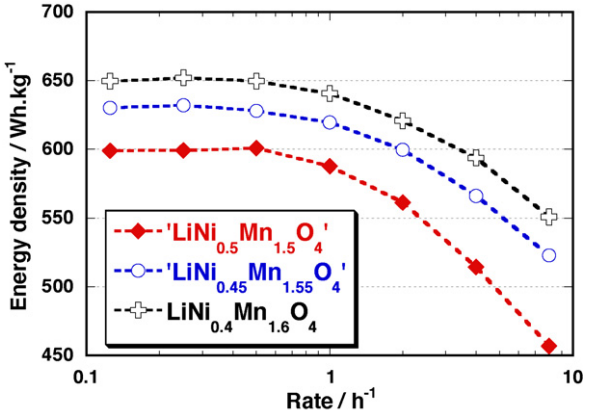

Fig. 7. Energy density as a function of cycle rate for $LiNi_{0.4}Mn_{1.6}O_4$, '$LiNi_{0.45}Mn_{1.55}O_4$' and '$LiNi_{0.5}Mn_{1.5}O_4$' tested in lithium coin cell at 20 °C, between 3.5 and 5 V vs. Li^+/Li.

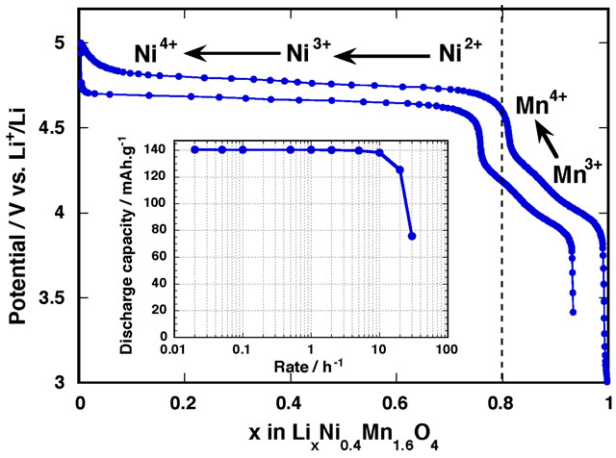

Fig. 8. Potential–composition profile of $LiNi_{0.4}Mn_{1.6}O_4$ spinel oxide vs. lithium at *C*/5 rate at 20 °C. (Insert) Specific capacity vs. discharge rate.

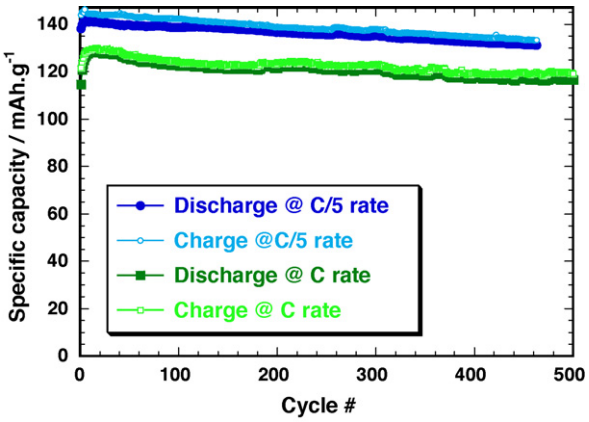

Fig. 9. Specific capacity vs. cycle number for the $LiNi_{0.4}Mn_{1.6}O_4$/Li system at *C* and *C*/5 rates at 20 °C.

ity fading, thus to increase the cycle life of the batteries, several authors reported the benefit of using particle coating. Zinc oxide coating of the surface of $LiNi_{0.5}Mn_{1.5}O_4$ particles was the most popular solution to reduce the interface reactivity of this material [13–16]. Aqueous solution containing zinc acetate and spinel oxide was used to prepare coated sample (<5 wt.% of coating), before further drying and heating. It seems that ZnO acts as getter of the in situ formed HF molecules (produced by electrolyte degradation), known to be detrimental for the cycle-ability. Almost no capacity fading for 50 cycles results from zinc oxide coating. No result under high rate has been reported so far. Silver coated-$LiNi_{0.5}Mn_{1.5}O_4$ was also presented [17], and showed to be not satisfactory for extended cycling. This was partly explained by the ability to form insulating Ag_2O coating during first charge. A more exotic study has been realized by Kobayashi et al. on an all solid state composite lithium battery, with Li_3PO_4-coated-$LiNi_{0.5}Mn_{1.5}O_4$ [18]. The authors show that Li_3PO_4 coating unambiguously improve 5 V cycling of polymer electrolyte (Li_3PO_4 forms a stable interface between the positive electrode and the solid polymer electrolyte), but results are still far away from those using conventional liquid electrolyte. Like announced in the experimental section, we realized a post-synthesis treatment, different from previous authors, of the as prepared materials in aqueous solution to get better electrochemical performances, particularly the cycle life. From now, all the results presented below are obtained on post-treated $LiNi_{0.4}Mn_{1.6}O_4$ materials. The electrochemical profile and rate capability of the $LiNi_{0.4}{}^{2+}Mn_{0.2}{}^{3+}Mn_{1.4}{}^{4+}O_4$/Li system are reported in Fig. 8. One fifth of the capacity is due to the oxidation of Mn^{3+} ions, and four fifth to the oxidation of Ni^{2+}. Reaction of this high voltage spinel oxide with lithium is reversible with a low first cycle irreversibility. The insert graph expresses the very high rate capability of this spinel oxide (diffusion of Li^+ ions is usually fact for spinel oxides due to the presence of interconnected channels in the 3D structure). Nominal capacity is preserved up to 10*C* rate (~140 mAh g^{-1}). Extended cycling at full charge/discharge is presented in Fig. 9. Results obtained at 20 °C at *C*/5 and 1*C* rates are very promising, with 0.015% loss of capacity per cycle. In these conditions, the cycle life (i.e., corresponding to a 20% loss of capacity) is well above 1000 cycles, despite the inherent thermodynamic instability of common electrolyte solvents above 4.5 V vs. Li^+/Li.

To be able to assemble high energy density Li-ion prototypes, we had to optimize the active material environment by controlling the formulation and the elaboration process of electrode. The best compromise gives electrodes containing 90% $LiNi_{0.4}Mn_{1.6}O_4$, with a part for additives (binder and carbon) minimized to 10% by weight (it was 20% for our conventional thin electrodes discussed above). Reversible capacities are 124–129 mAh g^{-1} for all loadings (Fig. 10). The loss of capacity is very small and the polarization is only increased in a small amount when comparing thinner and thicker electrodes. Average discharge potential is 4.43–4.49 V vs. Li^+/Li. The first cycle irreversible capacity is rather low (3.1–3.8%), and practical gravimetric energy densities are in the 560–580 Wh kg^{-1} of material range. Tests in Li-ion coin cell, using graphite at the negative electrode, will be presented below in order to take advantage of the good performances of high loaded positive electrode.

Finally, we have verified by ex situ X-ray measurements that the $LiNi_{0.4}Mn_{1.6}O_4$/$Ni_{0.4}Mn_{1.6}O_4$ redox couple is highly reversible from a structural point of view. Even after more than 500 cycles at 100% state of charge/discharge, we checked that the structure and the crystallinity of the electrode material are preserved. Good thermal reactivity at high state of charge was also demonstrated. We noticed by differential scanning calorimetry measurements that delithiated high voltage nickel manganese spinel oxides are less reactive than layered oxides toward the electrolyte (same order than the well-know stable $LiFePO_4$). We are confident that the above observations definitely give evidence of the possibility to use high voltage spinel oxides as positive electrode in Li-ion batteries. The materials retain most part of their capacity at high rate and their cycle life is remarkable. Specific advantages of using $LiNi_{0.4}Mn_{1.6}O_4$ have been given. However, some limitations due to the electrolyte instability have to be circumvented.

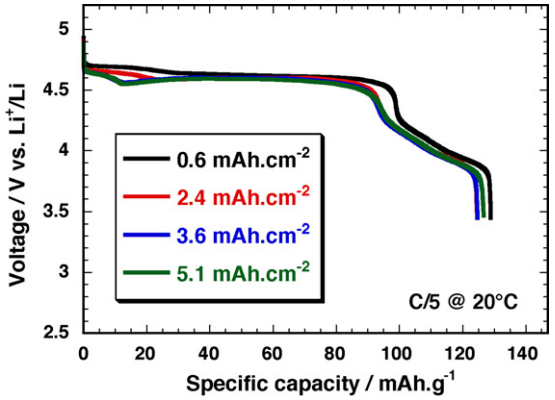

Fig. 10. Voltage–composition profile in discharge of electrodes containing 90% $LiNi_{0.4}Mn_{1.6}O_4$ (various loading) under galvanostatic mode at *C*/5 rate at 20 °C.

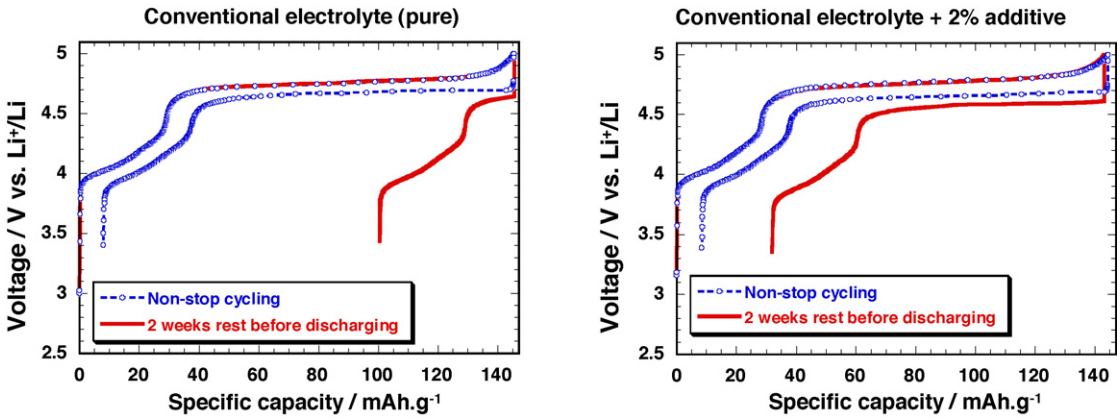

Fig. 11. Effect of a specific additive tested to reduce the self-discharge at high voltage for the $LiNi_{0.4}Mn_{1.6}O_4$/Li system (coin cell with 0.4 mAh cm^{-2} electrode containing 80% active material, 10% Super P and 10% binder). Conventional electrolyte is $LiPF_6$ (1 M) in EC/PC/DPC (1/1/3). Cycling was performed at *C*/5 at 20 °C. Both systems have similar "non-stop" cycling profile. After open circuit voltage for 2 weeks, restored capacity is 150% more important when additive is used (18% self-discharge vs. 68%).

3.3. Electrolyte

To our knowledge, there is no usable electrolyte for cycling correctly above 4.5 V vs. Li^+/Li. Conventional electrolytes, like $LiPF_6$ salt dissolved in carbonate mixtures, give reactive electrode/electrolyte interface at high voltages. In consequence, the self-discharge is rapid at high voltage. Varying the scan rate (e.g., *C*/100) or the temperature (e.g., 55 °C) also shows the existence of a competing electrochemical process (charge capacity is higher than the theoretical value corresponding to the extraction of all lithium ions from '$LiNi_{0.5}Mn_{1.5}O_4$' or $LiNi_{0.4}Mn_{1.6}O_4$). This phenomenon does not affect the cycle life in cells with metallic lithium counter electrode and excess of electrolyte. But it should consume electrolyte, generate self-discharge and disrupt the Li balancing within both electrodes of a Li-ion system. This is why it is unavoidable to work to the stabilization of the electrode/electrolyte interface.

Following the work done on the carbon negative electrode in the 1990's (introduction of small amount of vinylidene carbonate (VC) in the electrolyte), it is interesting to form a stable solid electrolyte interface (SEI) on the positive electrode side. This approach, not widespread until now for the positive electrode, is being followed by Ube Industries in Japan [19]. In an exploratory approach, we recently initiated a first evaluation of the impact of several additives on the self-discharge that could initiate in situ coating during initial charge by decomposition of the additive. Some of the organic families we have investigated for the moment are sultones, alkyl acetates, phenyls and alkyl phosphites. Promising results have been obtained with the 1-3 propane sultone additive. In the best case, a reduction of the self-discharge by a factor of three to four has been observed with only 2% additive (Fig. 11), thus giving interest to this original approach for further development. In the normal conditions described in the experimental section (thin electrode containing 10% weight Super P carbon), approximately two third of the capacity is lost after 2 weeks in open circuit voltage at high voltage (−68%). With the best additive evaluated for the moment, the self-discharge was reduced to only 16% in 2 weeks. Coulombic efficiency, corresponding to the discharge over charge capacity ratio, is usually between 97 and 98%. It reaches 99% at C or *C*/5 rate with additive. An other possibility to reduce the self-discharge consists in reducing the global specific surface area of conductive grains. During our optimization for improving the performance of thick electrodes, to be used in high capacity Li-ion cells, we showed that electrode with only 2% high surface area Super P carbon has 2.5 times lower self-discharge than the conventional thin electrodes.

The developments and future studies to be realized on the high voltage spinel oxides must be dedicated to the minimization of the surface reactivity of the compound towards the electrolyte, while maintaining high kinetic properties. Other additives that could protect all active surfaces in contact with electrolyte will be tested, together with an investigation of new ionic liquids and solvents. Present results are already promising and would allow to evaluate the interest in high voltage nickel manganese spinel oxides in Li-ion batteries.

4. Discussion

4.1. '5 V' high energy Li-ion cells

Since the introduction on the market of the first Li-ion cell by Sony in the early 90's, worldwide researches have been performed to find better active materials (capacity, cost, safety, cyclability, efficiency, stability, self-discharge, etc.) to face increasing power source demand. By technological progresses, energy density was improved from less than 100 Wh kg^{-1} in 1991 to more than 200 Wh kg^{-1} in 2008. Numerous applications like mobile phones, laptops, handy terminals/PDAs, digital (video) cameras, Bluetooth devices, portable DVDs, satellites communication devices, scooters, Segway and electric vehicles are all expecting for new high (volumetric and gravimetric) energy density Li-ion batteries. Weight of active materials at the positive and negative electrodes has large impact of the global gravimetric cell energy density, with more than 50% out of the total. Other cell components are casing, separator, binders, electronic conductors, electrolyte, etc. At present, the prime solution to reduce the global weight consists in improving the active materials performances (capacity and/or potential). In addition, the weight of active material at the negative electrode is less than 40% of the weight of active material at the positive electrode. It means that the impact of the positive electrode on the cell gravimetric energy density is more important than the negative counterpart. For volumetric energy density, the negative electrode has almost similar impact than the positive electrode.

Today, carbon (graphite) is the evident choice for the negative electrode. In our case, the active material is a mixture of mesocarbon microbeads (MCMB, Osaka gas) with synthetic flake graphite (SFG, Timcal) and homemade carbon micro-fibers, representing 96% of the total weight. Binder, essentially carboxymethyl cellulose (CMC, Aldrich), is 4%. We believe that this electrode formulation offers a good compromise between mechanical strength and elec-

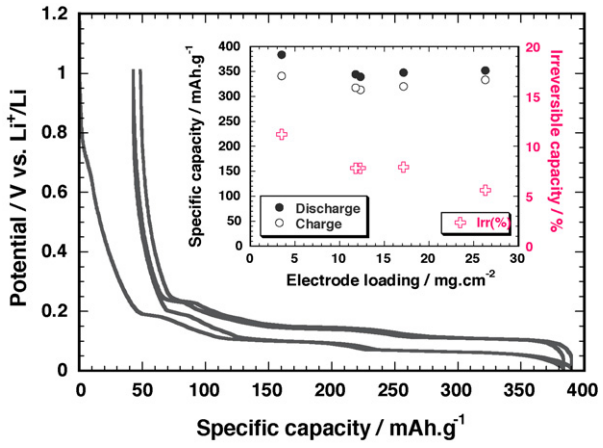

Fig. 12. Voltage–capacity profile under galvanostatic mode at *C*/20 at 20 °C for thin carbon electrode (3.8 mg cm^{-2}). (Insert) Specific capacity and first cycle irreversible capacity of carbon electrodes (*C*/20 rate at 20 °C).

trochemical performances. Reversible capacity is high and first cycle irreversibility is low (Fig. 12, coin cell). Cycle life is also as good as expected. It was been tested on thin electrodes vs. lithium (lithium foil is rapidly damaged for superior current densities by unit area) and on thick electrodes vs. a commercial positive electrode.

Combination of high voltage spinel oxides with carbon is generalized by the reaction below: $LiNi_{0.4}Mn_{1.4}O_4 + C_6 \leftrightarrow Li_{1-x}Ni_{0.4}Mn_{1.6}O_4 + Li_xC_6$. In practice, graphite has usually to be employed in excess to balance the irreversible loss of capacity due to the formation of the passivation layer at the negative electrode, and to prevent lithium deposition at the end of charge. On the contrary, high voltage materials should be used in excess in order to protect the electrolyte against excessive oxidation. For these reasons, no excess was selected. As for most of the commercial energy Li-ion cell, electrodes loading are in the 3.5–4.5 mAh cm^{-2} range. Fig. 13 reports the electrochemical profile of a 2 A h Li-ion cell based on the $LiNi_{0.4}Mn_{1.6}O_4$/carbon system (the 3rd cycle is reported). Main features of the prototype are indicated within the graph. Energy density is already rather satisfactory (~220 Wh kg^{-1} at the 3rd cycle), letting us to hope for a rapid success (240 Wh kg^{-1}) in the future. At the opposite, cycle life has to be improved, because more than 20% of the capacity is lost during the first 100 cycles. Note that we observed small manganese dissolution after prolonged cycling on lithium coin

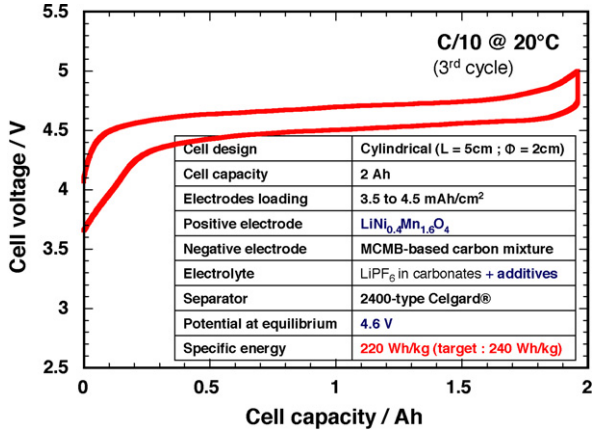

Fig. 13. Charge/discharge profile (third cycle) of a 2 A h $LiNi_{0.4}Mn_{1.6}O_4$/carbon prototype obtained at *C*/10 rate at 20 °C. Features of the cell are reported in the graph.

cell. This has almost no effect on a lithium foil, but it could have much more detrimental effect on a graphite negative electrode (low cycle life).

4.2. '3 V' safe and high power Li-ion cells

Some applications like power tools, R/Cs (models, toys), HEVs, PHEVs require high power batteries. For example, the HEVs currently use Nickel–Metal Hydride batteries (Ni–MH). This technology is now stabilized, and no important improvement can be expected. Ni–MH batteries sustain several limitations, such as a power density limited to ~1.3 kW kg^{-1}, a low power at low temperature, a charge efficiency seriously weakened above 50 °C, a moderate cycle life, and a cost strongly dependent on the increasing price of nickel and cobalt. That will require – in the view of the car manufacturers – the advent of a different type of batteries in the future. The Li-ion technology is already seriously considered as a promising storage system for automotive applications. Security is a crucial issue for these large size mobile applications and it is still a weak point for the present Li-ion technology that should be resolved in a near future with the use of new cell components. Li-ion batteries have already been integrated in car prototypes. A mass production requires the replacement of the conventional $LiCoO_2$-type positive electrode for safety and cost reasons. Among possible alternatives, we believe that the high voltage spinel oxides give the possibility to reach high energy densities and high power with higher safety and lower cost than $LiCoO_2$. For high power Li-ion cell, carbon could be also a limiting factor due to the possibility to form unsafe lithium dendrites. High power Li-ion batteries, using $Li_4Ti_5O_{12}$ at the negative electrode to replace carbon, have been regarded in the last few years [20,21]. The choice of the lithium titanate was dictated by the numerous advantages of this new alternative negative electrode material over graphite. $Li_4Ti_4O_{12}$ is a zero-strain material [22], which would confer almost unlimited cycle life. Moreover, the operating voltage is constant at 1.55 V vs. Li^+/Li, preventing electrolyte degradation (solvent reduction during the first discharge) and lithium plating. In other words, $Li_4Ti_5O_{12}$ is recommended for high rate applications.

Work on the $LiNi_{0.5}Mn_{1.5}O_4/Li_4Ti_5O_{12}$ redox couple has naturally been published by Professor Ohzuku, announcing a retention of capacity as high as 83% after 1100 cycles [23,24]. In collaboration with Ohzuku et al. Amazutsumi, from SANYO, recently presented a communication on the $LiNi_{0.5}Mn_{1.5}O_4/Li_4Ti_5O_{12}$ system [25]. This presentation of the most famous battery manufacturer confirmed the interest in such a system. In our laboratory, we have also made similar investigation for the last few years. $Li_4Ti_5O_{12}$ was prepared by homemade process [26]. More recently, we have decided to embark on the study of TiO_2 for competing with $Li_4Ti_5O_{12}$. In particular, TiO_2–B is a really interesting crystal form of titanium dioxide due to its opened-framework that favours lithium insertion. This compound was reported for the first time in 1980 by Marchand [27]. The synthesis consists in three consecutive steps, starting with the preparation of $K_2Ti_4O_9$ by solid state reaction. This precursor is subsequently hydrolysed in acidic condition to form $H_xTi_4O_9{\cdot}nH_2O$ compound. Final heat treatment gives TiO_2–B. Since 2004, Bruce's group published numerous papers on the hydrothermal synthesis of TiO_2–B nanowires and nanotubes, and their reactivity with lithium [28,29]. Depending on the method (original or hydrothermal) and conditions (temperature, time, pH, concentration, etc.), we elaborated TiO_2–B with various morphologies and size. Electrochemical performances, particularly the profile and the specific capacity, are extensively modified. The theoretical capacity of $TiO_2/LiTiO_2$ is 335 mAh g^{-1}. In comparison, it is 175 mAh g^{-1} for $Li_4Ti_5O_{12}/Li_7Ti_5O_{12}$ at almost similar voltage (Fig. 14). TiO_2–B does not present a long two-phase plateau like for $Li_4Ti_5O_{12}$. Moreover,

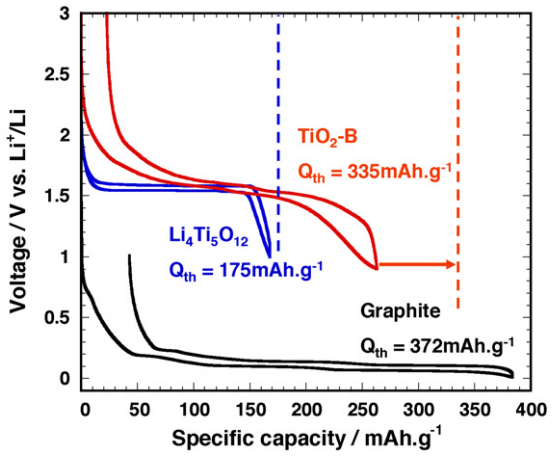

Fig. 14. Voltage vs. capacity for three negative electrode materials (conventional graphite vs. homemade $Li_4Ti_5O_{12}$ vs. homemade TiO_2–B), obtained under normal cycling conditions (20 °C, *C*/20 rate). For this figure (and next figure), homemade TiO_2–B powder synthesized according to the original process of Marchand [27] has been used.

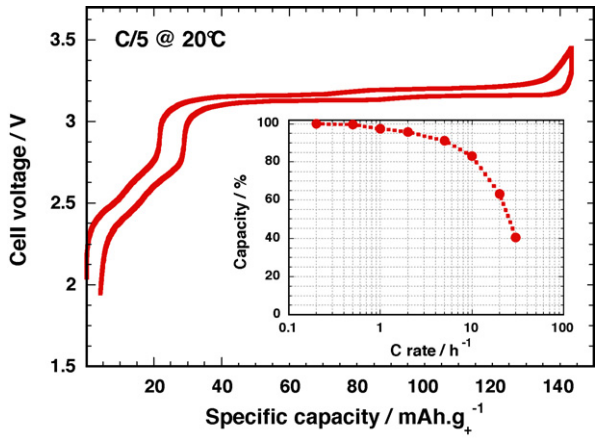

Fig. 16. Charge–discharge profile of a $LiNi_{0.4}Mn_{1.6}O_4/Li_4Ti_5O_{12}$ cell obtained under galvanostatic mode at *C*/5 rate at 20 °C. (Insert) Rate capability curve.

the drop of potential, from approximately 2 to 1 V vs. Li^+/Li, can be adjusted with the elaboration process of the material. This could be interesting for an easy control of the state of charge. In practice, TiO_2–B has higher capacity than $Li_4Ti_5O_{12}$ at low rate. Rate capability of both materials vs. lithium is reported in Fig. 15. Up to 10*C* rate, TiO_2–B sustains higher capacity than $Li_4Ti_5O_{12}$. However, the capacity retention from *C*/10 to 10*C* is 55% for the former, and 65–70% for the latter. Further experiments should be dedicated to master this weakness to really benefit from the advantages of TiO_2–B.

We examined the reaction of high voltage oxides with $Li_4Ti_5O_{12}$. Contrary to conventional cells with graphite, there is no need to overload the negative electrode. A small excess of positive electrode might be used. For pure $LiNi_{0.5}Mn_{1.5}O_4$, the system exhibits a flat charge–discharge voltage profile at 3.15 V (only oxidation of Ni^{2+} into Ni^{4+}, balanced by reduction of Ti^{4+} into Ti^{3+}). For $LiNi_{0.4}Mn_{1.6}O_4$, and other Mn^{3+} containing samples, part of the reaction occurs at ca. 2.55 V (Fig. 16). The reversible reaction is summarized by the following equation: $3LiNi_{0.4}Mn_{1.6}O_4 + Li_4Ti_5O_{12} \leftrightarrow 3Li_{1-x}Ni_{0.4}Mn_{1.6}O_4 + Li_{4+3x}Ti_5O_{12}$, with $0 \le x \le 1$. Discharge capacity is stable at 137–139 mAh g^{-1} referring to $LiNi_{0.4}Mn_{1.6}O_4$, similar to the results with lithium coin cell. Loss of capacity is 0.06% per cycle, intermediate between our results with lithium and carbon negative electrode. It corresponds to a cycle life of about 300 cycles. Rate capability is very good for electrode loading to 1 mAh cm^{-2}, with 85% of the nominal capacity recovered at 10*C* rate. After the original work of Ohzuku on the '3 V' $LiNi_{0.5}Mn_{1.5}O_4/Li_4Ti_5O_{12}$ system [23,24], we confirm that the high voltage nickel manganese spinel oxides are suitable for high rate applications, particularly in discharge (charge cut-off voltage is only a few tens of milliVolts above the 3.15 V plateau).

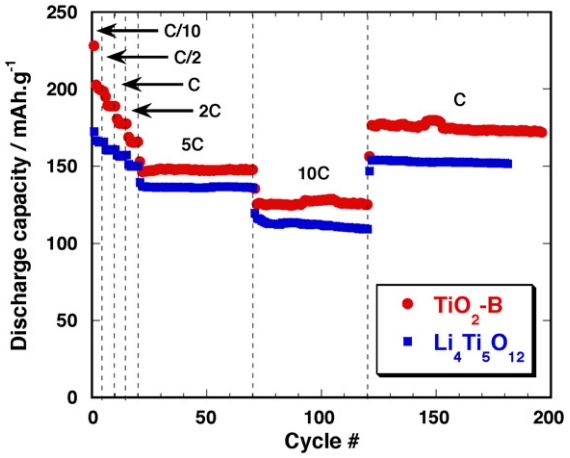

Fig. 15. Comparison of the discharge capacity vs. cycle number for TiO_2–B/Li and $Li_4Ti_5O_{12}$/Li systems at various rates (from *C*/10 to 10*C*).

5. Conclusion

Better knowledge of the distribution of Li, Mn and Ni atoms in the spinel sites was obtained from the neutron diffraction experiments. In particular, we confirmed the success to synthesize a pure and fully ordered $LiNi_{0.5}Mn_{1.5}O_4$ spinel oxide. We showed that the disordered samples contain partial ordering and $Li_xNi_{1-x}O$ impurities. By taking no particular precaution, the $LiNi_{0.4}Mn_{1.6}O_4$ material has no impurity. Optimization of the synthesis conditions gives good electrochemical performances. Although the post-treatment does not modify the X-ray and neutron diffraction patterns, it does improve the cycle life, probably by acting on the electrode/electrolyte interface. $LiNi_{0.4}Mn_{1.6}O_4$ composition is a high voltage and high rate capability insertion material. It is an attractive positive electrode material for next generations of Li-ion batteries, either for '5 V' high energy cells or for '3 V' safe and high power cells. However, the development of cells using high voltage insertion material is still challenging due to the inherent instability of electrolyte solvents. In the next months, we intend to continue the selection of additives in the electrolyte to protect the interface. Other complementary approaches, consisting in the replacement of conventional liquid carbonates with new solvents or the replacement of the conventional electrolyte with ionic liquid will also be favoured. Solving the problem of electrolyte instability at high voltage (above 4.5 V vs. Li^+/Li) is a real challenge that could definitely introduce the Li-ion technology in the vehicle application. It should also pave the way for researches on new materials (above 5 V vs. Li^+/Li) and new applications. For the moment, we are convinced that $LiNi_{0.4}Mn_{1.6}O_4$ and derivatives are promising materials for future high energy density and high power Li-ion batteries.

Acknowledgements

This work was partially supported by the European Space Agency under contract #20044/06/NL/JD. The authors thank Dr.

Evelyne Simon (ESA), Dr. Yvan Reynier (CEA) and Dr. Lucas Sannier (previously at CEA) for fruitful discussions, and Agnès Brun (CEA) for technical support. Clemens Ritter and the Institut Laue Langevin in Grenoble (France) are acknowledged for neutron diffraction data recording.

References

[1] J.M. Tarascon, E. Wang, F.K. Shokoohi, W.R. McKinnon, S. Colson, J. Electrochem. Soc. 138 (1991) 2859–2864.
[2] K. Amine, H. Tukamoto, H. Yasuda, Y. Fujita, J. Electrochem. Soc. 143 (1996) 1607–1613.
[3] K. Amine, H. Tukamoto, H. Yasuda, Y. Fujita, J. Power Sources 68 (1997) 604–608.
[4] Q. Zhong, A. Bonakdarpour, M. Zhang, Y. Gao, J.R. Dahn, J. Electrochem. Soc. 144 (1997) 205–213.
[5] WinPLOTR software, developed by T. Roisnel and J. Rodriguez-Carvajal, is downloadable at: http://www-llb.cea.fr/fullweb/winplotr/winplotr.htm; the FullProf suite is downloadable at: http://www.ill.eu/sites/fullprof/.
[6] D. Gryffroy, R.E. Vandenberghe, E. Legrand, Mater. Sci. Forum 79–82 (1991) 785–790.
[7] K. Takahashi, M. Saitoh, M. Sano, M. Fujita, K. Kifune, J. Electrochem. Soc. 151 (2004) A173–A177.
[8] J.-H. Kim, S.-T. Myung, C.S. Yoon, S.G. Kang, Y.-K. Sun, Chem. Mater. 16 (2004) 906–914.
[9] K. Ariyoshi, Y. Iwakoshi, N. Nakayama, T. Ohzuku, J. Electrochem. Soc. 151 (2004) A296–A303.
[10] J.H. Kim, C.S. KYoon, S.T. Myung, J. Prakash, Y.K. Sun, Electrochem. Solid-State Lett. 7 (2004) A216–A220.
[11] M. Kunduraci, G.G. Amatucci, Electrochim. Acta 53 (2008) 4193–4199.
[12] M. Kunduraci, J.F. Al-Sharab, G.G. Amatucci, Chem. Mater. 18 (2006) 3585.
[13] R. Alcantara, M. Jaraba, P. Lavela, J.L. Tirado, J. Electroanal. Chem. 566 (2004) 187–192.
[14] Y.-K. Sun, C.S. Yoon, I.-H. Oh, Electrochim. Acta 48 (2003) 503–506.
[15] Y.-K. Sun, K.-J. Hong, J. Prakash, K. Amine, Electrochem. Commun. 4 (2002) 344–348.
[16] Y.-K. Sun, Y.-S. Lee, M. Yoshio, K. Amine, Electrochem. Solid-State Lett. 5 (2002) A99–A102.
[17] J. Arrebola, A. Caballero, L. Hernán, J. Morales, E. Rodríguez Castellón, Electrochem. Solid-State Lett. 8 (2005) A303–A307.
[18] Y. Kobayashi, H. Miyashiro, K. Takei, H. Shigemura, M. Tabuchi, H. Kageyama, T. Iwahori, J. Electrochem. Soc. 150 (2003) A1577–A1582.
[19] K. Abe, Y. Ushigoe, H. Yoshitake, M. Yoshio, J. Power Sources 153 (2006) 328.
[20] Altairnano company, website: http://www.altairnano.com;; L. Kavan, J. Prochazka, T.M. Spitler, M. Kalba, M. Zukalova, T. Drezen, M. Graetzel, J. Heyrovsky, J. Electrochem. Soc. 150 (2003) A1000–A1007.
[21] EnerDel company, website: http://enerdel.com.
[22] T. Ohzuku, A. Ueda, N. Yamamoto, J. Electrochem. Soc. 142 (1995) 1431–1435.
[23] K. Ariyoshi, S. Yamamoto, T. Ohzuku, J. Power Sources 119–121 (2003) 959–963.
[24] T. Ohzuku, K. Ariyoshi, S. Yamamoto, Y. Makimura, Chem. Lett. 30 (2001) 1270–1271.
[25] T. Amazutsumi, K. Ariyoshi, T. Ohzuku, Three-volt Lithium-ion Battery Consisting of Li[Ni1/2Mn3/2]O4 and Li[Li1/3Ti5/3]O4, in: Proceedings of the 14th International Meeting on Lithium Batteries, Tianjin, 2008.
[26] S. Jouanneau, F. Le Cras, C. Bourbon and H. Lignier, Commissariat à l'Energie Atomique, patent # WO2006/027449.
[27] R. Marchand, L. Brohan, M. Tournoux, Mater. Res. Bull. 15 (1980) 1129–1133.
[28] A.R. Armstrong, G. Armstrong, J. Canales, P.G. Bruce, Angew. Chem. 43 (2004) 2286–2288.
[29] A.R. Armstrong, G. Armstrong, J. Canales, P.G. Bruce, Chem. Commun. (2005) 2454–2456.